MNRAS **000**, 1–8 (2015) Preprint 16 November 2015 Compiled using MNRAS LATEX style file v3.0

Cassiopeia A and direct Urca cooling

G. Taranto,[1,2] G. F. Burgio,[1] and H.-J. Schulze[1]
[1]*INFN Sezione di Catania, Via Santa Sofia 64, 95123 Catania, Italy*
[2]*Dipartimento di Fisica e Astronomia, Università di Catania, Via Santa Sofia 64, 95123 Catania, Italy*

16 November 2015

arXiv:1511.04243v1 [nucl-th] 13 Nov 2015

ABSTRACT
We model neutron star cooling, in particular the current rapid cooldown of the neutron star Cas A, with a microscopic nuclear equation of state featuring strong direct Urca processes and using compatible nuclear pairing gaps as well as effective masses. Several scenarios are possible to explain the features of Cas A, but only large and extended proton $^1S_0$ gaps and small neutron $^3PF_2$ gaps are able to accommodate also the major part of the complete current cooling data. We conclude that the possibility of strong direct Urca processes cannot be excluded from the cooling analysis.

Key words: stars: neutron – dense matter – equation of state.

1 INTRODUCTION

With the commissioning of increasingly sophisticated instruments, more and more details of the very faint signals emitted by neutron stars (NS) can be quantitatively monitored. This will allow in the near future an ever increasing accuracy to constrain the theoretical ideas for the ultra-dense matter that composes these objects.

One important tool of analysis is the temperature-vs.-age cooling diagram, in which currently a few (~ 20) observed NS are located. NS cooling is over a vast domain of time (10^{-10} – 10^5 yrs) dominated by neutrino emission due to several microscopic processes (Yakovlev et al. 2001; Page & Reddy 2006; Page et al. 2006; Lattimer & Prakash 2007). The theoretical analysis of these reactions requires the knowledge of the elementary matrix elements, the relevant beta-stable nuclear equation of state (EOS), and, most important, the superfluid properties of the stellar matter, i.e., the gaps and critical temperatures in the different pairing channels.

Even assuming (without proper justification) the absence of exotic components like hyperons and/or quark matter, the great variety of required input information under extreme conditions, that is theoretically not well under or out of control, renders the task of providing reliable and quantitative predictions currently extremely difficult.

Recently this activity has been spurred by the observation of very rapid cooling of the supernova remnant Cas A, of current age 335 years and surface temperature $T \approx 2 \times 10^6$ K, for which different analyses deduce a temperature decline of about 2 to 5 percent during the last ten years (Ho & Heinke 2009; Heinke & Ho 2010; Elshamouty et al. 2013). Mass and radius of this object are not directly observed, but in recent works optimal values $M = 1.62\,M_\odot$, $R \approx 10.2$ km (Elshamouty et al. 2013) or a range $M = (1.1-1.7)\,M_\odot$, $R \approx (11.4-12.6)$ km (Ho et al. 2015) are reported, dependent on the assumed EOS.

Two major theoretical scenarios have been proposed to explain this observation: One is to assume a fine-tuned small neutron 3PF2 (n3P2) gap, $T_c \approx (5-9) \times 10^8$ K $\sim \mathcal{O}(0.1\,\mathrm{MeV})$ (Page et al. 2011; Yakovlev et al. 2011; Shternin et al. 2011), that generates strong cooling at the right moment due to the superfluid neutron pair breaking and formation (PBF) mechanism (Page et al. 2009); the other one is based on a strongly reduced thermal conductivity of the stellar matter that delays the heat propagation from the core to the crust to a time compatible with the age of Cas A (Blaschke et al. 2012, 2013). Both explanations have in common that they exclude the possibility of large ($\gtrsim 0.1$ MeV) n3P2 gaps; in the first case because the corresponding critical temperature of the PBF process has to match the current internal temperature of Cas A; in the second case because such a gap would block too strongly the modified Urca (MU) cooling of the star and therefore lead to a too high temperature of Cas A.

Some alternative scenarios have also been brought forward. Amongst them, it was suggested in (Bonanno et al. 2014) that the fast cooling regime observed in Cas A can be explained if the Joule heating produced by dissipation of the small-scale magnetic field in the crust is taken into account. A further explanation was proposed in (Sedrakian 2013), according to which the enhancement of the neutrino emission is triggered by a transition from a fully gapped two-flavor color-superconducting phase to a gapless/crystalline phase, although such a scenario requires a very massive $\sim 2M_\odot$ star.

A common feature of all these cooling scenarios is that they exclude from the beginning the possibility of very fast direct Urca (DU) cooling, although many microscopic nuclear EOS do reach easily the required proton fractions for this process (Li & Schulze 2008; Burgio & Schulze 2010; Li et al. 2012; Taranto et al. 2013); and we will employ in this work an EOS that does so. However, the Akmal-Pandharipande-Ravenhall (APR) variational EOS (Akmal et al. 1998), which is perhaps the most frequently used EOS for cooling simulations (Gusakov et al. 2005; Page et al. 2011; Yakovlev et al. 2011; Shternin et al. 2011; Blaschke et al. 2012, 2013), (in spite of the fact that it does not reproduce the em-

© 2015 The Authors

pirical saturation point of nuclear matter without an ad-hoc correction), features a rather low proton fraction and DU cooling only sets in for very heavy neutron stars, $M \gtrsim 2M_{\odot}$. Since in any case neither this nor any other EOS can currently be experimentally verified or falsified at high density, the frequent use of one particular EOS represents an important bias that should not be underestimated.

Another critical point of most current cooling simulations is the fact that EOS and pairing gaps are treated in disjoint and inconsistent manner, i.e., a given EOS is combined with pairing gaps obtained within a different theoretical approach and using different input interactions.

In this work we try to improve on both aspects, i.e., we include the DU cooling process predicted by our microscopic nuclear EOS, and we use compatible nuclear pairing gaps obtained with exactly the same nuclear (in-medium) interaction. Furthermore, we also employ recent results for nucleon effective masses obtained in the same approach with the same interactions (Baldo et al. 2014), which affect the microscopic cooling reactions.

This paper is organized as follows. In Section 2 we give a brief overview of the Brueckner-Hartree-Fock (BHF) theoretical framework adopted for the EOS, whereas in Section 3 pairing gaps obtained in the same framework and with the same interaction, will be introduced. Section 4 is devoted to the discussion of several scenarios for Cas A cooling, taking into account different choices for superfluid gaps and thermal conductivity. Conclusions are drawn in Section 5.

2 EQUATION OF STATE

Our EOS is determined within the BHF theoretical approach for nuclear matter (Jeukenne et al. 1976; Baldo 1999; Baldo & Burgio 2012), which computes the in-medium G-matrix nucleon-nucleon (NN) interaction from the bare NN potential V,

$$G[\rho;\omega] = V + \sum_{k_a k_b} V \frac{|k_a k_b\rangle Q \langle k_a k_b|}{\omega - e(k_a) - e(k_b)} G[\rho;\omega]\,, \tag{1}$$

where $\rho = \sum_{k<k_F}$ is the nucleon number density, and ω the starting energy. The single-particle (s.p.) energy

$$e(k) = e(k;\rho) = \frac{k^2}{2m} + U(k;\rho) \tag{2}$$

and the Pauli operator Q determine the propagation of intermediate baryon pairs. The BHF approximation for the s.p. potential $U(k;\rho)$ using the *continuous choice* prescription is

$$U(k;\rho) = \mathrm{Re} \sum_{k'<k_F} \left\langle kk' \middle| G[\rho; e(k)+e(k')] \middle| kk' \right\rangle_a , \tag{3}$$

where the subscript a indicates antisymmetrization of the matrix element, and the energy per nucleon is then given by

$$\frac{E}{A} = \frac{3}{5}\frac{k_F^2}{2m} + \frac{1}{2\rho}\sum_{k<k_F} U(k;\rho)\,. \tag{4}$$

In this scheme, the only input quantity needed is the bare NN interaction V in the Bethe-Goldstone equation (1), supplemented by a suitable three-nucleon force (TBF) in order to reproduce correctly the saturation properties of nuclear matter. In this work we use the Argonne V_{18} NN interaction (Wiringa et al. 1995) and the Urbana-type UIX TBF (Carlson et al. 1983; Schiavilla et al. 1986; Pudliner et al. 1997) as input. The results for the EOS including numerical parametrizations can be found in (Burgio & Schulze 2010; Taranto et al. 2013). We also reiterate that in the cooling simulations we employ neutron and proton effective masses,

$$\frac{m^*(k)}{m} = \frac{k}{m}\left[\frac{de(k)}{dk}\right]^{-1}, \tag{5}$$

derived consistently from the BHF s.p. energy $e(k)$, Eq. (2), (Baldo et al. 2014). Although the effect is not large compared to other uncertainties regarding the cooling, such a consistent treatment is hard to find in previous works. The model just described will be denoted by "BHF" in the following and some confrontation with the "APR" model (Akmal et al. 1998), which is based on the same input interactions, will be made. We use here the original APR "$A18+\delta v+\mathrm{UIX}^*$ corrected" results (Akmal et al. 1998) and not one of the parametrized versions (Heiselberg & Hjorth-Jensen 2000; Gusakov et al. 2005), where the high-density behavior is arbitrarily modified.

In fact we compare in Fig. 1 the NS EOS obtained with the APR and BHF models, i.e., panels (a) and (b) show pres-

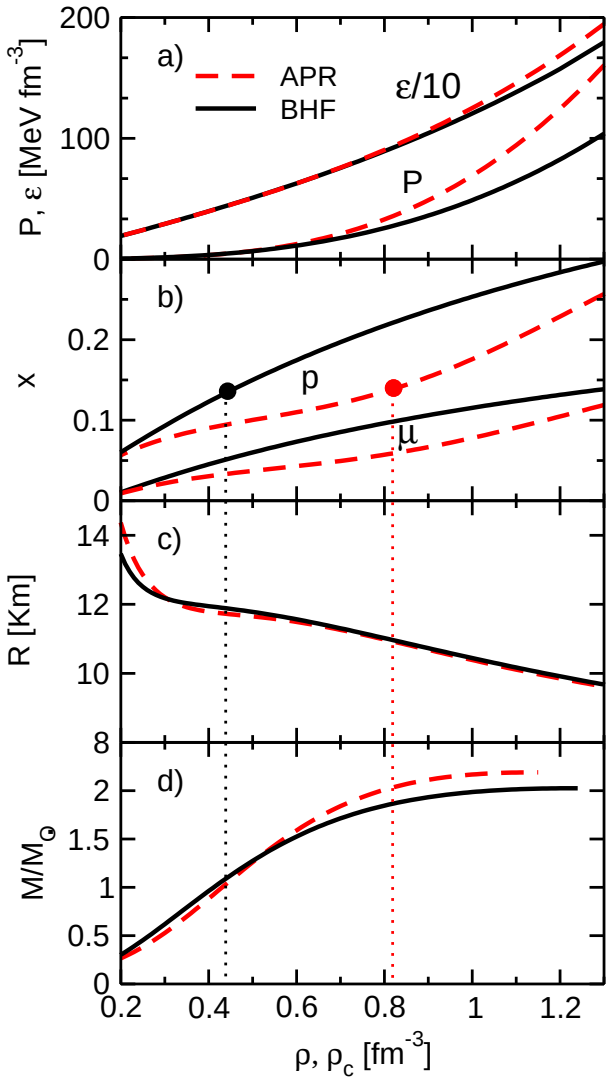

Figure 1. (Color online) Pressure and energy density (a), and proton and muon fractions (b) as functions of baryon number density ρ in beta-stable matter for the APR and BHF EOS. The lower panels show neutron star mass (d) and radius (c) as functions of the central density ρ_c. The DU onset is indicated by vertical dotted lines.

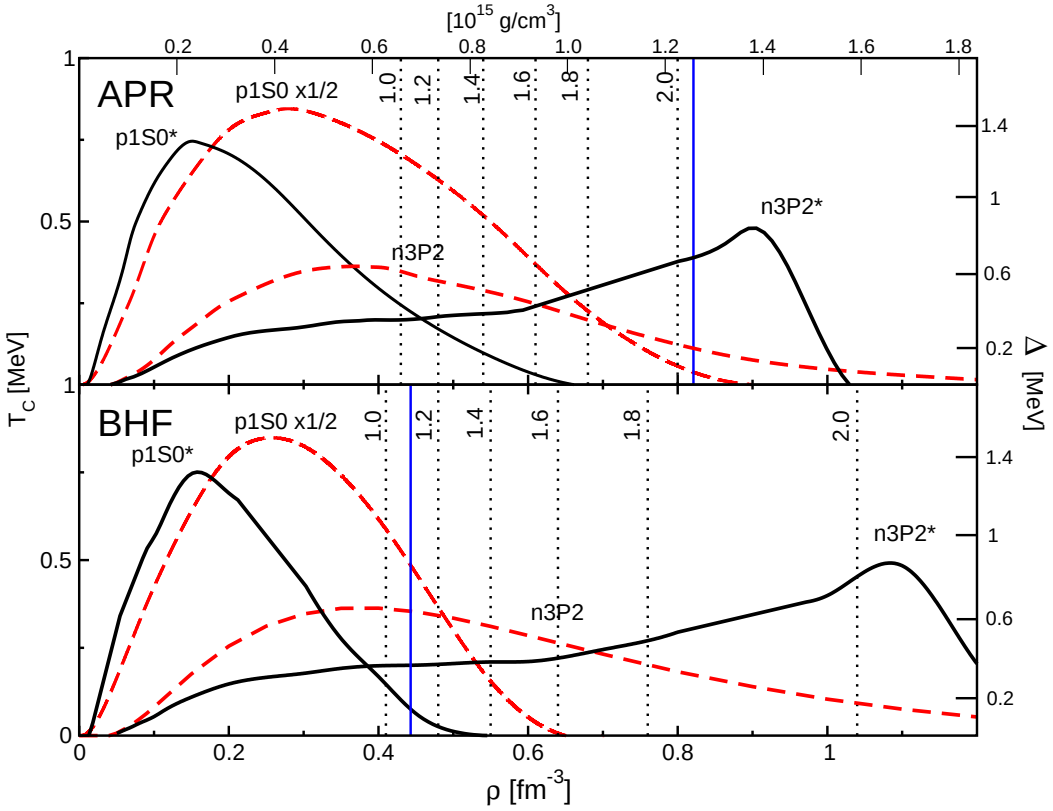

Figure 2. (Color online) Pairing gaps in NS matter for the APR and BHF models in the p1S0 and n3P2 channels, including (*) or not effective mass effects. Vertical dotted lines indicate the central density of NS with different masses $M/M_\odot = 1.0,\ldots,2.0$. DU onset occurs at the vertical solid (blue) lines. Note the scaling factor 1/2 for the p1S0 curves.

sure, energy density, and proton and muon fractions of beta-stable and charge-neutral matter as functions of the baryon density. It is obvious that the crucial difference between both models is the much higher proton fraction in the BHF approach. In this case the DU threshold is already reached at $\rho = 0.44\,\mathrm{fm}^{-3}$ ($x_p = 0.136$), whereas with the APR it is delayed to $\rho = 0.82\,\mathrm{fm}^{-3}$ ($x_p = 0.140$).

On the contrary, the APR EOS is somewhat stiffer, i.e., features a larger pressure and energy density. We also mention that the APR EOS becomes superluminal at $\rho = 0.85\,\mathrm{fm}^{-3}$, whereas BHF remains always below the critical threshold (Burgio & Schulze 2010; Taranto et al. 2013).

By solving the standard Tolman-Oppenheimer-Volkov equations for the NS structure, this input yields the NS (mass,radius) – central density relations shown in panels (c) and (d) of Fig. 1. We remark that both models reach maximum masses (slightly) above two solar masses and predict very similar radii in spite of their different matter composition. With BHF the DU process is active in nearly all stars, $M/M_\odot > 1.10$, while with APR only in the most heavy ones, $M/M_\odot > 2.03$. This has profound consequences for the cooling behavior.

3 PAIRING GAPS AND CRITICAL TEMPERATURES

Of vital importance for any cooling simulation is the knowledge of the 1S0 and 3PF2 pairing gaps for neutrons and protons in beta-stable matter, which on one hand block the DU and MU reactions, and on the other hand open new cooling channels by the PBF mechanism for stellar matter in the vicinity of the critical temperature (Yakovlev et al. 2001). As usual, we focus in this work on the most important proton 1S0 (p1S0) and neutron 3PF2 (n3P2) pairing channels and neglect the less important remaining combinations.

As stressed before, the gaps should be computed in a framework that is consistent with the determination of the EOS, i.e., be based on the same NN interaction and using the same medium effects (TBF and effective masses), and indeed we follow this procedure here, by using the results of (Zhou et al. 2004), which employed the same V18+UIX nuclear interaction and BHF s.p. spectra for the calculation of the gaps. To be more precise, and focusing on the more general case of pairing in the coupled 3PF2 channel, the pairing gaps were computed on the BCS level by solving the (angle-averaged) gap equation (Amundsen & Østgaard 1985; Baldo et al. 1992; Takatsuka & Tamagaki 1993; Elgarøy et al. 1996; Khodel et al. 1998; Baldo et al. 1998) for the two-component $L = 1,3$ gap function,

$$\begin{pmatrix}\Delta_1\\ \Delta_3\end{pmatrix}(k) = -\frac{1}{\pi}\int_0^\infty dk' k'^2 \frac{1}{E(k')}\begin{pmatrix}V_{11} & V_{13}\\ V_{31} & V_{33}\end{pmatrix}(k,k')\begin{pmatrix}\Delta_1\\ \Delta_3\end{pmatrix}(k') \tag{6}$$

with

$$E(k)^2 = [e(k)-\mu]^2 + \Delta_1(k)^2 + \Delta_3(k)^2\,, \tag{7}$$

while fixing the (neutron or proton) density,

$$\rho = \frac{k_F^3}{3\pi^2} = 2\sum_k \frac{1}{2}\left[1 - \frac{e(k)-\mu}{E(k)}\right]. \tag{8}$$

Here $e(k)$ are the BHF s.p. energies, Eq. (2), containing contribu-

tions due to two-body and three-body forces, $\mu \approx e(k_F)$ is the (neutron) chemical potential determined self-consistently from Eqs. (6–8), and

$$V_{LL'}(k,k') = \int_0^\infty dr\, r^2\, j_{L'}(k'r)\, V_{LL'}^{TS}(r)\, j_L(kr) \qquad (9)$$

are the relevant potential matrix elements ($T=1$ and $S=1$; $L,L'=1,3$ for the 3PF2 channel, $S=0$; $L,L'=0$ for the 1S0 channel) with

$$V = V_{18} + \bar{V}_{\rm UIX}\,, \qquad (10)$$

composed of two-body force and averaged TBF.

The relation between (angle-averaged) pairing gap at zero temperature $\Delta \equiv \sqrt{\Delta_1^2(k_F)+\Delta_3^2(k_F)}$ obtained in this way and the critical temperature of superfluidity is then $T_c \approx 0.567\Delta$.

Fig. 2 displays the p1S0 and n3P2 pairing gaps as a function of baryonic density of beta-stable matter for the APR (upper panel) and BHF (lower panel) models. Also indicated are the central densities of NS with different masses, in order to easily identify which range of gaps is active in different stars. Note that the in-medium modification of the pairing interaction is treated consistently (via the compatible s.p. energies and TBF) only in the BHF model.

In (Zhou et al. 2004) different levels of approximation for the calculation of gaps were discussed, in particular one including only the two-body force V_{18} in Eq. (10) together with the kinetic s.p. energies, and another one (curves denoted by p1S0* and n3P2* in Fig. 2) using the BHF s.p. spectra according to Eq. (2). Note that polarization corrections (Lombardo & Schulze 2001; Sedrakian & Clark 2006; Baldo & Schulze 2007; Gandolfi et al. 2008) were not considered in that work, which for the case of the 1S0 channel are known to be repulsive, but for the 3PF2 are still essentially unknown, and might change the value of the gaps even by orders of magnitude (Khodel et al. 2004; Schwenk & Friman 2004; Ding et al. 2015). In order to represent this uncertainty, we use in the cooling simulations the density dependence of the pairing gaps shown in Fig. 2, but employ global scaling factors s_p and s_n, respectively.

Qualitatively one observes in Fig. 2 the natural scaling effect of the different proton fractions for the BHF and APR EOS, such that the p1S0 gaps extend to larger (central) densities for the APR model, due to the lower proton fraction in that case. Therefore the blocking effect on the cooling extends up to higher densities and NS masses for the APR model. The crucial difference is again the onset of the DU process, which is active for nearly all NS in the BHF case. However, the n3P2$^{(*)}$ gaps extend up to very large density and can thus provide an efficient means to block this cooling process, in particular for the n3P2* model comprising medium effects. The price to pay is an enhanced PBF cooling rate close to the critical temperature in that case. Note that the 3P2 gaps shown in the figure are larger than those currently employed in cooling simulations, which will be discussed in the next section, and that at the moment there exists no satisfactory theoretical calculation of p-wave pairing that includes consistently all medium effects.

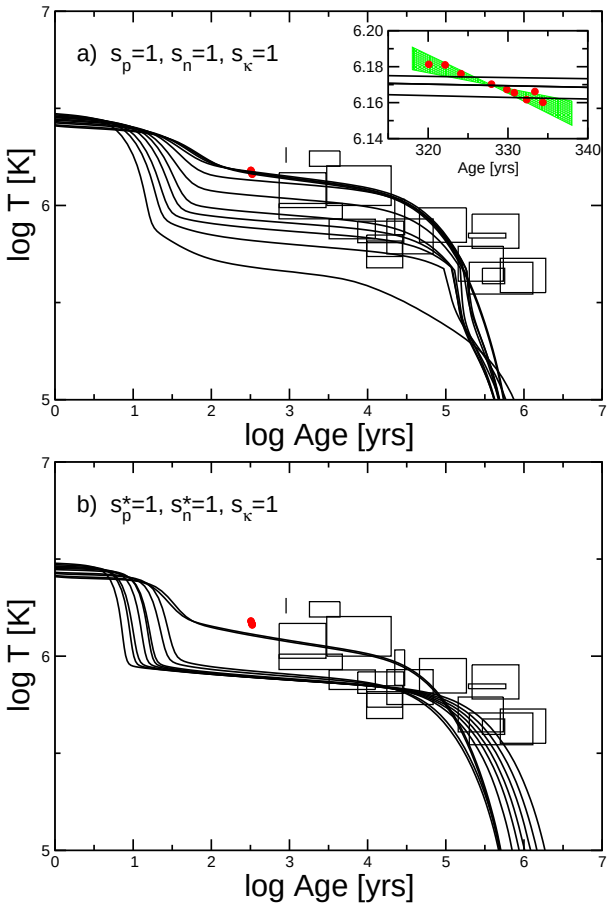

Figure 3. (Color online) Cooling curves with the BHF EOS and no scaling factors, for different NS masses $M/M_\odot = 1.0, 1.1, \ldots, 2.0$ (decreasing curves). The upper panel employs BCS gaps with free s.p. spectra, whereas in the lower panel the BHF s.p. spectra are used. Red dots show the Cas A cooling data (enlarged in the inset of the upper panel; the $M/M_\odot$ =1.1 and 1.2 curves overlap).

4 NEUTRON STAR COOLING AND CAS A

Having quantitatively specified EOS and pairing gaps, the NS cooling simulations are carried out using the widely used code `NSCool` (Page 2010), which comprises all relevant cooling reactions: DU, MU, PBF, and Bremsstrahlung.

A further important ingredient of the simulations is the (leptonic and baryonic) thermal conductivity, and the default choice in (Page & Reddy 2006; Page et al. 2006; Page 2010) is to use the results of (Gnedin & Yakovlev 1995; Yakovlev et al. 2001; Baiko et al. 2001). Recently it has been conjectured (Shternin & Yakovlev 2007, 2008; Blaschke et al. 2012, 2013) that the conductivities could be substantially (by one order of magnitude) suppressed by in-medium effects, and this has been put forward as an alternative explanation of the rapid Cas A cooling. We follow this idea by introducing a further global scale factor s_κ multiplying the total thermal conductivity. Therefore our calculations are controlled by the three global parameters s_p, s_n, s_κ, and we present now some selected results for certain parameter choices.

Our set of observational cooling data comprises the (age, temperature) information of the 19 isolated NS sources listed in (Beznogov & Yakovlev 2015a). We point out, however, the recent discovery of the unusually hot object XMMU J173203.3-344518 (Klochkov et al. 2015) with estimated age and temperature (10-40 kyr, 2.1-2.8 MK). We do not include it in our current analysis, as it is in fact incompatible with most previous cooling simulations, and will certainly be studied in great detail in the future.

4.1 Scenario 1: Original model, no scaling

For the sake of illustration and better understanding we begin by showing the results obtained with the original pairing gaps shown in Fig. 2, and without any modification of the conductivities, i.e., setting $s_p = s_n = s_k = 1$. Moreover we use the neutron $^1S_0$ BCS gap as calculated in (Zhou et al. 2004), without any rescaling, although the beta-stable matter in the relevant subnuclear density domain of the crust is inhomogeneous and therefore more elaborate considerations should be done (Pastore et al. 2011, 2013).

The upper panel of Fig. 3 shows the temperature vs age results (11 curves for NS with masses $1.0, 1.1, \ldots, 2.0$) obtained with the BCS gaps without any medium modification (dashed red curves in the lower panel of Fig. 2), while the lower panel employs the gaps with BHF effective masses (black curves in Fig. 2), which is indicated by the notation $s_p^* = s_n^* = 1$ here and in the following. In all cases a heavy (Fe) elements atmosphere ($\eta = 0$) has been assumed. One observes results in line with the features of the pairing gaps, namely in the upper panel light ($M \lesssim 1.4 M_\odot$) NS cool slower and heavy ($M \gtrsim 1.7 M_\odot$) NS cool faster than in the lower panel. This is due to the larger overall values of the corresponding BCS gaps in the low-density ($n \lesssim 0.6\,\mathrm{fm}^{-3}$) region and the smaller n3P2 value in the high-density ($n \gtrsim 0.7\,\mathrm{fm}^{-3}$) domain, see Fig. 2, which cause, respectively, a stronger or weaker blocking of the dominant DU process in light or heavy stars.

Very old and warm stars (PSR B1055-52, RX J0720.4-3125) (as well as the recent XMMU J1732) are not covered by any cooling curve, just as in the equivalent investigation within the APR model of (Page et al. 2009); and we refer to that article for a discussion of possible reasons. Altogether, our cooling curves for warm stars appear quite similar to those in that reference, while there is no difficulty at all to explain cold stars due to the DU mechanism in the BHF model. The main reason for the too low temperature of old stars is an early cooldown due to the n3P2 PBF process, as we shall see.

The major shortcoming of both scenarios in Fig. 3 is that they cannot reproduce the particular cooling properties of Cas A: While the first one can fit its current age and temperature as a $M = 1.2 M_\odot$ NS, neither reproduces the apparent very fast current cooldown (Ho & Heinke 2009; Heinke & Ho 2010; Elshamouty et al. 2013), shown in the inset of the upper panel. Precisely for this reason special scenarios with fine-tuned parameters have been developed, which we analyze now.

4.2 Scenario 2: Neutron pair breaking cooling

A frequent explanation of the rapid cooling of Cas A is the one based on an appropriately chosen n3P2 gap, which causes strong cooling due to the opening of the neutron PBF process at the current age/temperature of the star. The BHF EOS including strong DU reactions also allows this interpretation by choosing the scaling factors $s_p = 2.0$, $s_n = 0.132$, $s_\kappa = 1$ for a $1.4 M_\odot$ star, corresponding to maximum values of the gaps $\Delta_p \approx 6\,\mathrm{MeV}$ and $\Delta_n \approx 0.1\,\mathrm{MeV}$, i.e., Δ_p is larger than usually chosen (in order to block the fast DU reaction; the domain of the p1S0 gap fully covers NS up to about $1.6 M_\odot$, see Fig. 2), while Δ_n is in line with the equivalent results of (Ho et al. 2015; Page et al. 2011; Yakovlev et al. 2011; Shternin et al. 2011).

The results are shown in Fig. 4, which displays the sequence of cooling curves for NS masses $M/M_\odot = 1.0, 1.1, \ldots, 2.0$, the 1.4 case corresponding to Cas A by construction; (this might be changed within reasonable limits by choosing different scaling factors). In this case the neutron $^1S_0$ gap has been rescaled by a factor 0.04 for finetuning. As in similar investigations (Ho et al. 2015; Page et al. 2009), one notes that the rapid cooldown caused by the n3P2 PBF renders even more difficult the reproduction of old hot stars. Also for this reason alternative scenarios have been developed, and we analyze one of them now.

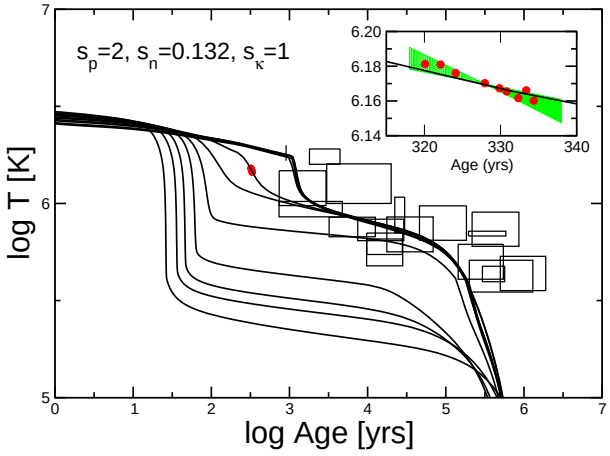

Figure 4. (Color online) Same as Fig. 3, for the PBF cooling scenario. The $M = 1.4 M_\odot$ cooling curve passes through Cas A by construction.

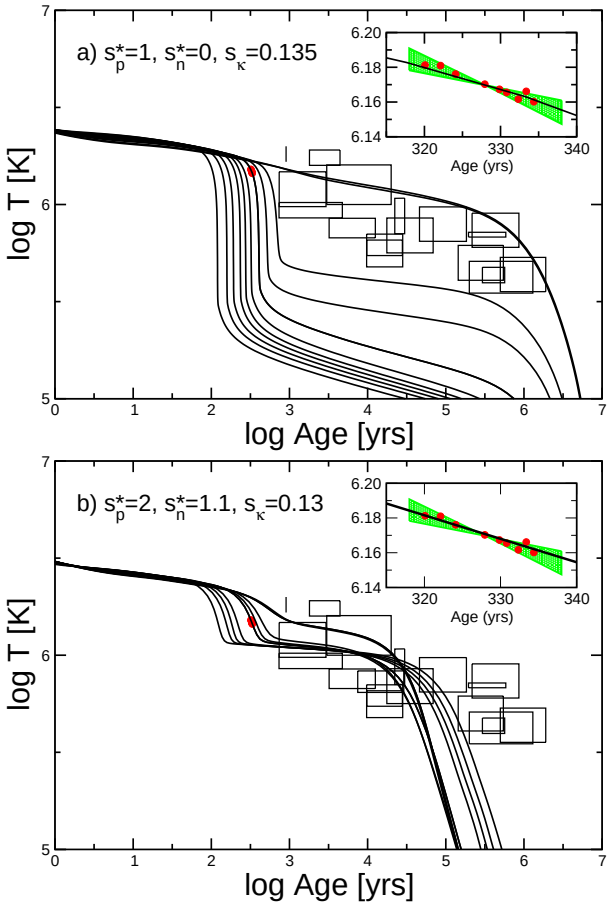

Figure 5. (Color online) Same as Fig. 4, for two delayed cooling scenarios.

4.3 Scenario 3: Suppressed thermal conductivity

The approach of (Blaschke et al. 2012, 2013) features strongly suppressed lepton and baryon thermal conductivities, which we roughly simulate by the scaling parameter s_κ, as in (Blaschke et al. 2012). [In (Blaschke et al. 2013) a more microscopic treatment of this reduction was introduced, which however did not lead to qualitatively different conclusions]. The reduced conductivity serves to delay the temperature decline up to the current age of Cas A without need to introduce fine-tuned nPBF cooling. A further peculiarity of this model is the fact that the standard MU cooling is strongly enhanced by assumed in-medium effects (MMU), which provides fast cooling for heavy NS, without need of DU cooling (Grigorian & Voskresensky 2005).

Our EOS including DU cooling also accommodates the possibility of reduced thermal conductivities, as demonstrated in Fig. 5. The upper panel shows a rather satisfactory fit of all cooling data including Cas A, employing the parameter set $s_p^* = 1$, $s_n^* = 0$, $s_\kappa = 0.135$, where the size of s_κ is comparable to the values of about 0.2 deduced in (Blaschke et al. 2012, 2013).

In this scenario a rather small value of the n3P2 gap seems to be required, as otherwise old hot (and also young cold) NS cannot be obtained, even if Cas A is reproduced. This is demonstrated by a typical result ($s_p^* = 2.0$, $s_n^* = 1.1$, $s_\kappa = 0.13$, the n1S0 gap has been reduced by 0.09, and $\eta = 0.03$ here), shown in the lower panel of the figure, where large values for both gaps are used. The features of Cas A are reproduced correctly, but the finite large n3P2 gap causes an early rapid cooldown incompatible with the temperature of most old NS, but at the same time together with the large p1S0 gap reduces too strongly the DU and MU cooling in order to fit young cold stars.

4.4 Scenario 4: No Cas A constraint

The previous results have demonstrated that it is difficult to satisfy simultaneously the rapid cooling of Cas A and the slow cooling of old NS, see Fig. 4 or Fig. 5(a), where the hottest stars are slightly missed. This is true not only in the current analysis (Page et al. 2009). However, recently doubts have been expressed about the validity of the Cas A data analysis (Posselt et al. 2013), such that a future revision towards much slower or no cooling at all is not excluded.

We therefore study finally a scenario without the Cas A constraint (apart from reproducing its current age and temperature with a reasonable mass) in our strong DU model, trying to cover the full range of current cooling data. Starting from the observation that the use of the unscaled BCS gaps in Fig. 3 yields already a reasonable reproduction of most young NS, and considering the fact that a finite n3P2 gap produces too strong PBF cooling, simply switching off this channel yields a nearly perfect coverage of all current cooling data, as shown in Fig. 6(b). In this scenario Cas A turns out a $1.31 M_\odot$ NS.

Thus the BCS p1S0 gap alone is able to suppress sufficiently the DU cooling, provided that it extends over a large enough density range. Since in our case the p1S0 gap is perhaps somewhat large (although this might be compensated by a different density shape), we finally investigate the effect of rescaling it with factors $s_p = 0.5$ and $s_p = 2$, shown in panels (a) and (c). It turns out that in both cases the quality of the cooling simulation remains excellent, just the predicted mass of Cas A is varying between $1.18 M_\odot$ and $1.46 M_\odot$. This illustrates the dire necessity of precise information on the masses of the NS in the cooling diagram, without which no theoretical cooling model can be verified.

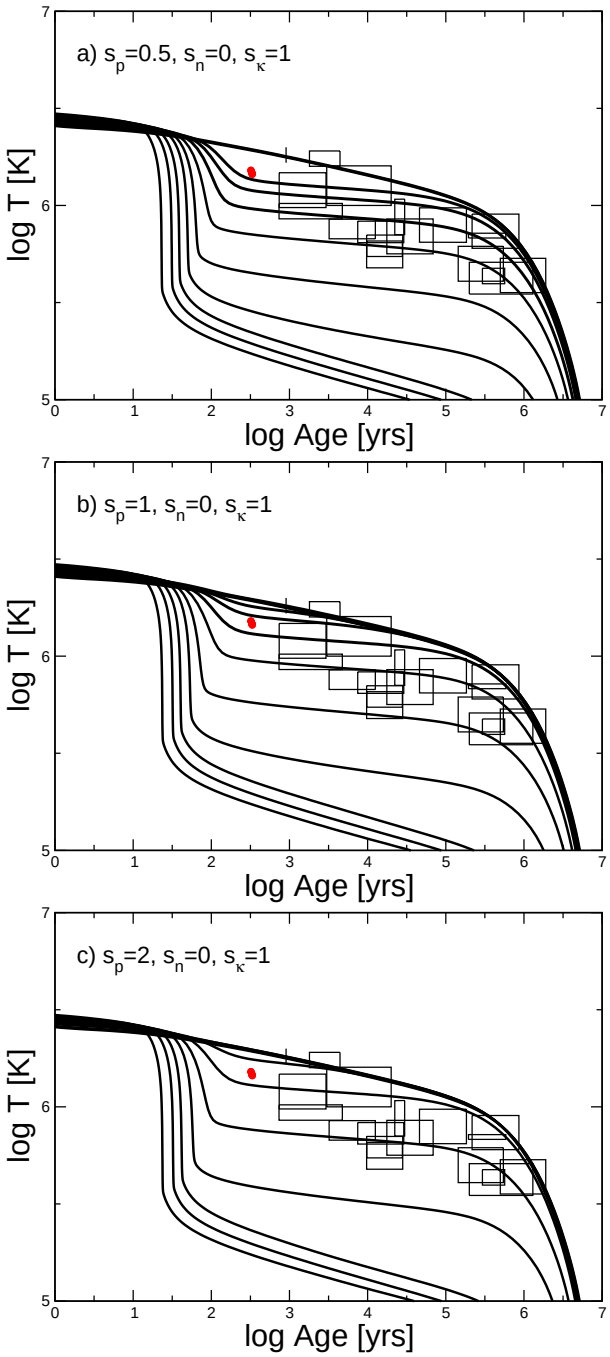

Figure 6. (Color online) Same as Fig. 3, using $s_n = 0$, $s_\kappa = 1$, and different choices of $s_p = 0.5, 1.0, 2.0$ (from top to bottom).

A further possible constraint for cooling models could be the statistical population synthesis $\log N - \log S$ analysis, which might exclude a very sudden early onset of unmasked DU cooling (Popov et al. 2006; Klähn et al. 2006; Blaschke & Grigorian 2007; Posselt et al. 2008, 2010; Beznogov & Yakovlev 2015a,b). A given cooling model, together with the position of the observed NS in the cooling diagram, makes a definite prediction for the mass spectrum of NS, which could be compared with empirical information. For example, a sudden onset of the DU process as in Fig. 5(a) causes a

strong variation of the cooling curve with increasing NS mass, and therefore a related enhancement of the deduced NS mass spectrum in that domain.

However, this method is currently still burdened with large uncertainties, in particular due to the unknown “true" mass distribution of NS and the difficult selection effect that makes too cold NS unobservable! Furthermore, in our calculation the DU process is strongly masked by the extended p1S0 gap, such that the transition to DU cooling is not very abrupt (see Fig. 6), and therefore an exclusion of this scenario might not be straightforward. Together with a better knowledge of NS masses, the population synthesis might however be a further efficient tool for the cooling analysis in the future.

5 CONCLUSIONS

We have studied NS cooling using a microscopic BHF EOS featuring strong direct Urca reactions setting in at $\rho = 0.44\,\mathrm{fm}^{-3}$, $M/M_\odot > 1.10$, and using compatible p1S0 and n3P2 pairing gaps as well as nucleon effective masses. The current substantial theoretical uncertainty regarding gaps and thermal conductivity was modelled in a rather simple way by introducing three global scale factors.

We found that it is possible to reproduce the apparent fast cooling of Cas A by either finetuning the n3P2 pairing gap or reducing the thermal conductivity. In general it is difficult to then simultaneously fit old hot NS, although we did find a suitable parameter set for that purpose.

Relaxing the Cas A constraint, it is astonishing to see how well all current cooling data can be fit by just assuming the p1S0 BCS gap (with some freedom of scaling) and a vanishing n3P2 gap.

Our results affirm the extreme difficulty to draw quantitative conclusions from the current NS cooling data containing no information on the masses of the cooling objects, due to the large variety of required microphysics input that is hardly known or constrained otherwise.

We have shown that not even the combination of very strong DU cooling with sufficiently large and extended p1S0 gaps and small n3P2 pairing gaps can be excluded. There is still ample freedom to choose the magnitude and shape of the p1S0 gap, as long as the covered density domain is sufficiently large in order to fully mask the DU onset up to sufficiently heavy stars. One can only hope to resolve this problem once precise information on the NS masses in the cooling diagram becomes available.

Even more exotic possibilities of blocking the DU process by strong p3P2 pairing (Zhou et al. 2004) are not excluded either, but were not analyzed in this work; as neither the effect of exotic components of matter (hyperons, quarks) that should appear at high density and completely change the theoretical picture (Page et al. 2000; Tsuruta et al. 2009). In any case there are strong indications from theoretical many-body calculations and supported by the current analysis, that the DU process becomes active at moderately high baryon density; it should thus never be excluded without justification in cooling simulations.

ACKNOWLEDGMENTS

We acknowledge useful discussions with M. Baldo, A. Bonanno, D. Page, and W. Ho. Partial support comes from “NewCompStar," COST Action MP1304.

REFERENCES

Akmal A., Pandharipande V. R., Ravenhall D. G., 1998, Phys. Rev. C, 58, 1804
Amundsen L., Østgaard E., 1985, Nuclear Phys. A, 442, 163
Baiko D. A., Haensel P., Yakovlev D. G., 2001, A&A, 374, 151
Baldo M., 1999, Int. Rev. Nucl. Phys., World Scientific, Singapore, vol.8,
Baldo M., Burgio G. F., 2012, Rep. Prog. Phys., 75, 026301
Baldo M., Schulze H.-J., 2007, Phys. Rev. C, 75, 025802
Baldo M., Cugnon J., Lejeune A., Lombardo U., 1992, Nuclear Phys. A, 536, 349
Baldo M., Elgarøy Ø., Engvik L., Hjorth-Jensen M., Schulze H.-J., 1998, Phys. Rev. C, 58, 1921
Baldo M., Burgio G. F., Schulze H.-J., Taranto G., 2014, Phys. Rev. C, 89, 048801
Beznogov M. V., Yakovlev D. G., 2015a, MNRAS, 447, 1598
Beznogov M. V., Yakovlev D. G., 2015b, MNRAS, 452, 540
Blaschke D., Grigorian H., 2007, Prog. Part. Nucl. Phys., 59, 139
Blaschke D., Grigorian H., Voskresensky D. N., Weber F., 2012, Phys. Rev. C, 85, 022802
Blaschke D., Grigorian H., Voskresensky D. N., 2013, Phys. Rev. C, 88, 065805
Bonanno A., Baldo M., Burgio G. F., Urpin V., 2014, A&A, 561, L5
Burgio G. F., Schulze H.-J., 2010, A&A, 518, A17
Carlson J., Pandharipande V., Wiringa R. B., 1983, Nuclear Phys. A, 401, 59
Ding D., Rios A., Dickhoff W. H., Dussan H., Polls A., Witte S. J., 2015, preprint, (arXiv:1502.05673)
Elgarøy Ø., Engvik L., Hjorth-Jensen M., Osnes E., 1996, Nuclear Phys. A, 607, 425
Elshamouty K. G., Heinke C. O., Sivakoff G. R., Ho W. C. G., Shternin P. S., Yakovlev D. G., Patnaude D. J., David L., 2013, ApJ, 777, 22
Gandolfi S., Illarionov A. Y., Fantoni S., Pederiva F., Schmidt K. E., 2008, Phys. Rev. Lett., 101, 132501
Gnedin O. Y., Yakovlev D. G., 1995, Nuclear Phys. A, 582, 697
Grigorian H., Voskresensky D. N., 2005, A&A, 444, 913
Gusakov M. E., Kaminker A. D., Yakovlev D. G., Gnedin O. Y., 2005, MNRAS, 363, 555
Heinke C. O., Ho W. C. G., 2010, ApJ, 719, L167
Heiselberg H., Hjorth-Jensen M., 2000, Phys. Rep., 328, 237
Ho W. C. G., Heinke C. O., 2009, Nature, 462, 71
Ho W. C. G., Elshamouty K. G., Heinke C. O., Potekhin A. Y., 2015, Phys. Rev. C, 91, 015806
Jeukenne J. P., Lejeune A., Mahaux C., 1976, Phys. Rep., 25, 83
Khodel V. A., Khodel V. V., Clark J. W., 1998, Phys. Rev. Lett., 81, 3828
Khodel V. A., Clark J. W., Takano M., Zverev M. V., 2004, Phys. Rev. Lett., 93, 151101
Klähn T., et al., 2006, Phys. Rev. C, 74, 035802
Klochkov D., Suleimanov V., Pühlhofer G., Yakovlev D. G., Santangelo A., Werner K., 2015, A&A, 573, A53
Lattimer J. M., Prakash M., 2007, Phys. Rep., 442, 109
Li Z. H., Schulze H.-J., 2008, Phys. Rev. C, 78, 028801
Li Z.-H., Zhang D.-P., Schulze H.-J., Zuo W., 2012, Chinese Physics Letters, 29, 012101
Lombardo U., Schulze H.-J., 2001, in Blaschke D., Glendenning N. K., Sedrakian A., eds, Lecture Notes in Physics, Berlin Springer Verlag Vol. 578, Physics of Neutron Star Interiors. p. 30 (arXiv:astro-ph/0012209)
Page D., 2010, NSCool code available at http://www.astroscu.unam.mx/neutrones/NSCool
Page D., Reddy S., 2006, Annual Review of Nuclear and Particle Science, 56, 327
Page D., Prakash M., Lattimer J. M., Steiner A. W., 2000, Phys. Rev. Lett., 85, 2048
Page D., Geppert U., Weber F., 2006, Nuclear Phys. A, 777, 497
Page D., Lattimer J. M., Prakash M., Steiner A. W., 2009, ApJ, 707, 1131
Page D., Prakash M., Lattimer J. M., Steiner A. W., 2011, Phys. Rev. Lett., 106, 081101

Pastore A., Baroni S., Losa C., 2011, Phys. Rev. C, 84, 065807
Pastore A., Margueron J., Schuck P., Viñas X., 2013, Phys. Rev. C, 88, 034314
Popov S., Grigorian H., Turolla R., Blaschke D., 2006, A&A, 448, 327
Posselt B., Popov S. B., Haberl F., Trümper J., Turolla R., Neuhäuser R., 2008, A&A, 482, 617
Posselt B., Popov S. B., Haberl F., Trümper J., Turolla R., Neuhäuser R., Boldin P. A., 2010, A&A, 512, C2
Posselt B., Pavlov G. G., Suleimanov V., Kargaltsev O., 2013, ApJ, 779, 186
Pudliner B. S., Pandharipande V. R., Carlson J., Pieper S. C., Wiringa R. B., 1997, Phys. Rev. C, 56, 1720
Schiavilla R., Pandharipande V., Wiringa R. B., 1986, Nuclear Phys. A, 449, 219
Schwenk A., Friman B., 2004, Phys. Rev. Lett., 92, 082501
Sedrakian A., 2013, A&A, 555, L10
Sedrakian A., Clark J. W., 2006, Nuclear Superconductivity in Compact Stars: BCS Theory and Beyond. World Scientific Publishing Co, p. 135
Shternin P. S., Yakovlev D. G., 2007, Phys. Rev. D, 75, 103004
Shternin P. S., Yakovlev D. G., 2008, Azh, 34, 675
Shternin P. S., Yakovlev D. G., Heinke C. O., Ho W. C. G., Patnaude D. J., 2011, MNRAS, 412, L108
Takatsuka T., Tamagaki R., 1993, Prog. Theor. Phys. Suppl., 112, 27
Taranto G., Baldo M., Burgio G., 2013, Phys. Rev. C, 87, 045803
Tsuruta S., Sadino J., Kobelski A., Teter M. A., Liebmann A. C., Takatsuka T., Nomoto K., Umeda H., 2009, ApJ, 691, 621
Wiringa R. B., Stoks V., Schiavilla R., 1995, Phys. Rev. C, 51, 38
Yakovlev D. G., Kaminker A. D., Gnedin O. Y., Haensel P., 2001, Phys. Rep., 354, 1
Yakovlev D. G., Ho W. C. G., Shternin P. S., Heinke C. O., Potekhin A. Y., 2011, MNRAS, 411, 1977
Zhou X.-R., Schulze H.-J., Zhao E.-G., Pan F., Draayer J. P., 2004, Phys. Rev. C, 70, 048802

This paper has been typeset from a TEX/LATEX file prepared by the author.